The Conformers of Hydroxyacetaldehyde

Yanping Fan, Lai Peng Leong, and Ryan P. A. Bettens*

Department of Chemistry, National University of Singapore, 3 Science Drive 3, Singapore 117543

Received: July 12, 2006; In Final Form: April 11, 2007

Both two and eighteen dimensional quantum diffusion Monte Carlo (DMC) calculations were used to study the isomers of hydroxyacetaldehyde. A total of four unique minima, and the transition states connecting them, were located. Both two and eighteen dimensional potential energy surfaces were generated and used in the DMC runs. The rotational constants for the global minimum were predicted for all experimentally identified isotopomers and an approximate equilibrium structure obtained by combining our theoretical results with the experimentally observed rotational constants. The results obtained for the remaining isomers indicate that not all of them can be isolated in the gas phase.

Introduction

Hydroxyacetaldehyde, (hydroxyethanal, glycolaldehyde, CH_2-OHCHO), an isomer of methyl formate and acetic acid, has been recently seen toward the Galactic center cloud Sgr B2(N) (Hollis, Lovas, and Jewell 2000).[1] Generally, it is believed that saturated molecules in hot cores are synthesized on interstellar dust grains in a low-temperature era. However the synthesis of glycolaldehyde is currently unknown toward its source. Several research groups have paid attention to glycolaldehyde, its origin in interstellar clouds,[2] oxidation,[3] and its reaction with the OH radical[4,5] both experimentally and theoretically.

Marstokk and Møllendal[6−8] first systematically studied the structure of glycolaldehyde in the gas phase but only observed one isomer. Their microwave measurements of the parent molecule and deuterated species as well as three other isotopic species also included the dipole moment. They pointed out that the cis form, denoted GM in this paper, is the most stable conformer based on low level theoretical calculations of three possible conformers, denoted here as GM, L1, and L3. Later, it was found that there was a fourth conformer of glycolaldehyde (cf. Figure 1), denoted in this work as L2, in the theoretical work of Antero et al.[9] Recently, Senent[10] studied the torsional spectrum and interconversion process between the four conformers at the MP2/cc-pVQZ level using a two-dimensional variational approach. In addition, Senent[10] computed the rotation parameters corresponding to respective conformers.

In this paper our main focus is on the implications of introducing the full dimensionality of the potential energy surface (PES) of hydroxyacetaldehyde in the identification and assignment of different conformers. Because hydroxyacetaldehyde is an 8-atom system the total number of nuclear degrees of freedom is 18. The only feasible technique available to study systems with such high dimensionality is Diffusion Monte Carlo (DMC), which is used throughout this work. Quantum DMC is now routinely used to solve for the ground-state nuclear wavefunction and has been applied to a wide variety of systems including the 30-dimensional intermolecular modes of the water hexamer[11] and 142 and 452 torsions of a bimolecular system.[12] Systems where no degrees of freedom have been frozen have also been studied. Examples include 9 dimensions for of FCH_3[13], and 12 dimensions for CH_5^+[14], and the water dimer.[15,16]

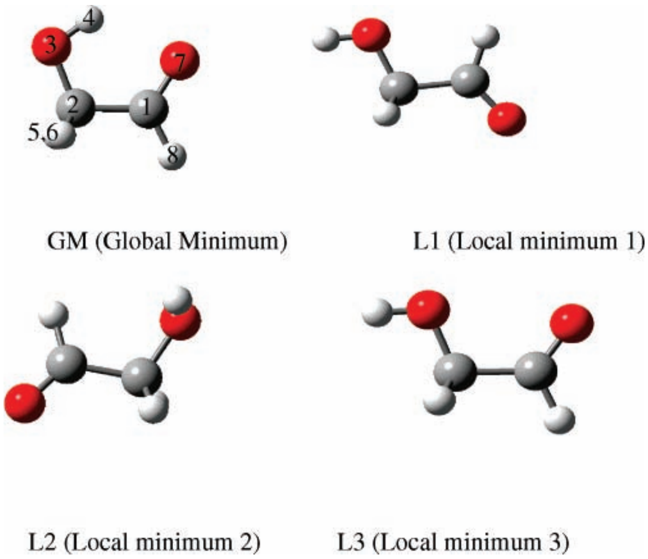

Figure 1. The four conformer structures of glycolaldehyde.

Methods

All ab initio calculations reported in this work were computed by using the Gaussian 98 suite of programs.[17] The PES was mapped in the two torsional angles, $\phi_1 = -OCCO$ and $\phi_2 = -HOCC$ by performing B3LYP/6-31G** constrained optimizations from $\phi_1 = -180-180$ in steps of 5° and $\phi_2 = 0-180$ in steps of 10°. That is, a total of 1387 constrained optimizations were performed. A contour plot of this two-dimensional PES is given in Figure 2. Indicated on this figure are all the minima and saddle points with the corresponding energies given in Scheme 1. Table 1 includes the energies of the minima at the B3LYP/6-31G(d,p), B3LYP/cc-pVTZ, CBS^{MP2}, and G3XMP2 levels.

Table 1 compares the four conformers energies at different levels of theory, the order is consistent for the two B3LYP calculations; however, the CBS^{MP2} and G3XMP2 methods both predict L1 to be slightly lower in energy than L2 as was also found by Senate.[10] The CBS calculations were performed in an

---

* To whom correspondence should be addressed. Email: chmbrpa@nus.edu.sg. Fax: +65 6779 1691.

10.1021/jp064408f CCC: $37.00

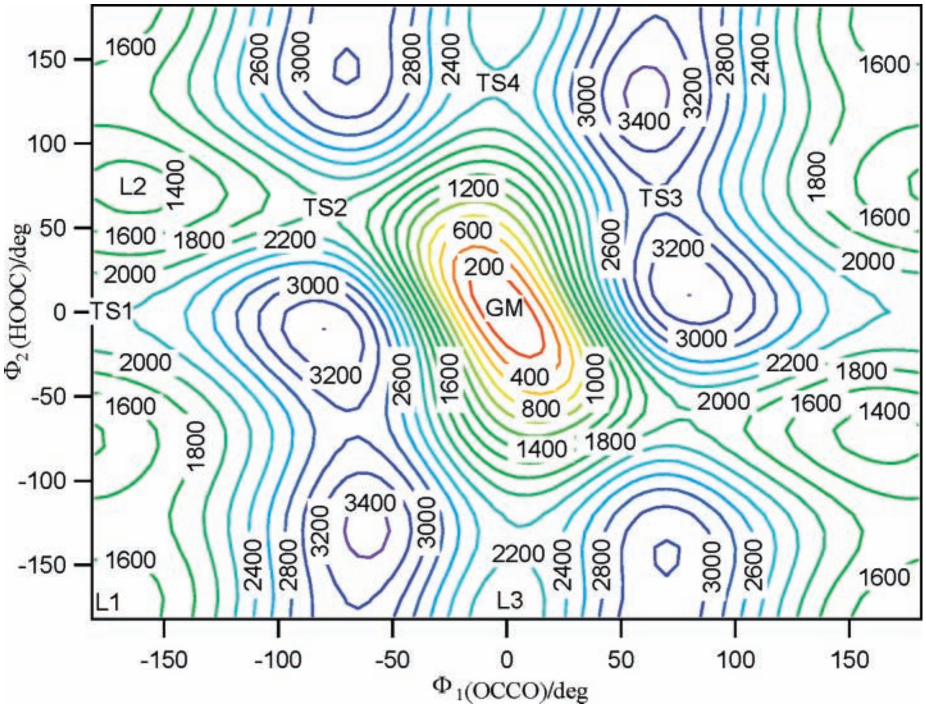

Figure 2. Contour plot of hydroxyacetaldehyde (energies in cm^{-1}) as a function of the two torsional angles.

SCHEME 1: Local Minima and Transition States for Hydroxyacetaldehyde at the B3LPY/6-31G Level of Theory**

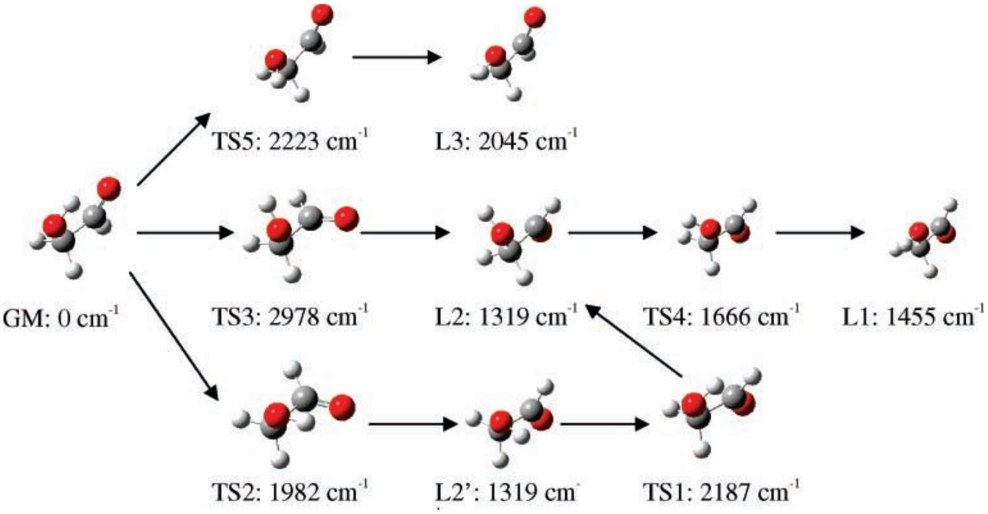

TABLE 1: Relative Energies (cm^{-1}) of Minima at the Various Levels of Theory

minima	B3LYP/6-31G(d,p)	Senent[a]	B3LYP/cc-pVTZ	CBS$_{MP2}$[b]	G3XMP2
GM	0	0	0	0	0
L1	1455	1278	1300	1260	1161
L2	1319	1297	1274	1340	1223
L3	2045	1865	1874	1860	1786
L3 → GM	178	175	158		
L2 → L2′	868	713	716		
L2 → L1	347	191	222		

[a] MP4(SDTQ)/cc-pVQZ//MP2/cc-pVQZ from ref 10. [b] MP2/aug-cc-pVXZ//MP2/aug-cc-pVTZ, X = T, Q and 5 energies were fit to $1/N^{1.5}$, where N was the number of basis functions. Relative energies from extrapolation accurate to ±20 cm^{-1}.

attempt to eliminate any basis set superpositioin error (BSSE) and to correctly describe the H-bond interaction. It is of note that the much higher level calculations agree reasonably well with the lower level B3LYP results. By combination of Table 1 and Scheme 1, it can be seen that L2 and L1 are very similar in energy and the barrier between them is small. Furthermore, the lowest barrier from conformer L3 to GM was calculated to be only 178 cm^{-1} at the B3LYP/6-31G(d,p) level and 175 cm^{-1} at the much higher level of Senent[10] (MP4-(SDTQ)/cc-pVQZ//MP2/cc-pVQZ). Our results and that of Senate both show that there exists a significant barrier between conformers L1 and the GM as well as L2 and the GM.

In DMC, small displacements are made to the Cartesian coordinates of the atoms. The size of the displacements depends on the mass of the nucleus and the imaginary time step size. As imaginary time passes the structure can change dramatically depending on the nature of the potential energy surface. In this work we ran DMC simulations on the B3LYP/6-31G(d,p) surface given in Figure 2 and an 18-dimensional surface derived from a subset of the grid points used to generate the two-dimensional surface, as described later.

In the two-dimensional calculations we have assumed that as the two torsional angles change the molecule is able to readjust its structure to the most stable form for the given values of ϕ_1 and ϕ_2. Hence after each time step we computed the two values of the torsional angles and then reset the remaining internal coordinates (and hence the structure) to an interpolation of the minimum energy structure that corresponded to these two angles. A simple bilinear interpolation was used to obtain the above internal coordinates based on the four sets of optimized internal coordinates, extracted from the grid described previously, that corresponded to the four bracketing pairs of ϕ_1 and ϕ_2. Similarly, a bilinear interpolation was also used to obtain the potential energy of the molecule for the given values of the torsional angles.

Here we specifically implemented discrete sampling DMC with 1000 initial replicas. The population was first pre-equilibrated using a step size of 5 au for 7000 steps in the 2-dimensional surface and 20000 steps on the 18-dimensional surface. After the pre-equilibration the zero-point energy was noted to have converged, and data sampling then occurred every 50 steps over a period of 10 000 steps using a step size of 1 au. The rotational constants were computed also during this period using the method of descendant weights. Descendants were followed for 1000 steps with a new set of descendants initiated and followed every 100 time steps. The reported results for the rotational constants are from 20 and 320 separate runs for the 2- and 18-dimensional surfaces, respectively. The reported errors are two standard deviations of the respective means.

To compute the rotational constants it is necessary to ensure that the Eckart conditions are enforced. A speedy algorithm was developed to ensure this and is essentially the same as that described by Kohn et al.[18] We also utilized the molecular symmetry of the system to effectively double the population size in computing the inverted moment of inertia tensor. Note that while we are always in the Eckart axis system, the inverted moment of inertia tensor is not exactly diagonal, except for the reference configuration. However, the absolute value of the off-diagonal elements for all isotopomers of the GM was never more than 21 MHz for the inverted product of inertia about the $a-b$ axes and never more than 2 MHz for the $a-c$ and $b-c$ axes.

We used two approaches for modeling the PES in 18 dimensions. One utilized the B3LYP/6-31G(d,p) level of theory, and the other the energies given by Senent[10] at the MP4(SDTQ)/cc-pVQZ level on the provided grid, but the first and second derivatives of the potential at these points at the B3LYP/6-31G-(d,p) level. At each of the grid points we performed constrained optimizations then obtained the energies, gradients, and second derivatives of the energy with respect to the coordinate system (described below). This data is then used in the Collins interpolation method[19] for evaluating the energy for any given configuration of the system in all 18 dimensions. We did apply one modification to standard Collins scheme, however, and that was to use $3n-6$ internal coordinates rather than the $n(n-1)/2$ interatomic distances. The following set of 18 internal coordinates were chosen (the atom labels can be found in Figure 1 for the GM), $\{r_1(C_1,C_2)$, $r_2(O_3,C_1)$, $r_3(H_4,C_1)$, $r_4(H_5,C_2)$, $r_5(H_6,C_2)$, $r_6(O_7,C_2)$, $r_7(H_8,O_7)$, $a_1(O_3,C_1,C_2)$, $a_2(H_4,C_1,C_2)$, $a_3(H_5,C_2,C_1)$, $a_4(H_6,C_2,C_1)$, $a_5(O_7,C_2,C_1)$, $a_6(H_8,O_7,C_2)$, $d_1(H_4,C_1,C_2,O_3)$, $d_2(H_5,C_2,C_1,H_4)$, $d_3(H_6,C_2,C_1,H_4)$, $d_4(O_7,C_2,C_1,O_3)$, $d_5(H_8,C_2,C_1,O_3)\}$, where r is an interatomic distance, a is bond angle, and d is dihedral angle. Note that $d_4 = \phi_1$ and $d_5 = \phi_2$. The Taylor series about each point of the surface was expanded in inverse r but directly in a and d. The above coordinate set transforms to the following set under the permutation-inversion operation of the molecular symmetry group of hydroxyacetaldehyde, i.e., the operation $(H_5,H_6)^*$, $\{r_1, r_2, r_3, r_5, r_4, r_6, r_7, a_1, a_2, a_4, a_3, a_5, a_6, -d_1, -d_3, -d_2, -d_5, -d_6\}$. Thus this choice of coordinates ensures that the potential possess the correct symmetry properties.

TABLE 2: Experimental Rotational Constants for Parent and Isotopomers of the Global Minimum Isomer Compared with the Perturbation Theory and DMC 2D and 18D Constants (Former Two Were Computed at the B3LYP/6-31G(d,p) Level, All Values Are in MHz)

	experiment[a]	exptl−perturb	exptl−DMC(2D)	exptl−fitted(18D)
			GM	
A	18446.4	106.5	−0.5 ± 1.0	−77.9 ± 17.6
B	6526.0	−52.8	25.1 ± 0.5	−3.6 ± 11.9
C	4969.3	−22.3	3.7 ± 0.2	7.4 ± 6.0
			CH_2OD-CHO	
A	17490.8	68.8	−3.4 ± 0.7	−47.7 ± 15.1
B	6499.8	−44.8	29.9 ± 0.4	−13.7 ± 11.7
C	4883.0	−18.9	4.7 ± 0.1	1.4 ± 5.8
			CH_2OH-CDO	
A	17151.3	103.0	16.0 ± 0.7	157 ± 18.1
B	6363.0	−47.7	26.5 ± 0.4	1.1 ± 9.3
C	4779.0	−18.3	4.1 ± 0.1	19.8 ± 6.1
			CHDOHCHO	
A	16988.0	104.1	14.5 ± 1.2	69.5 ± 17.4
B	6385.5	−51.0	20.5 ± 0.4	−19.0 ± 10.4
C	4843.8	−20.3	6.5 ± 0.2	13.0 ± 6.7
			$^{13}CH_2OH$-CHO	
A	18126.9	88.5	−13.9 ± 0.7	154.0 ± 19.5
B	6487.5	−49.9	26.5 ± 0.5	6.6 ± 11.5
C	4923.0	−22.4	2.8 ± 0.2	22.9 ± 7.4
			CH_2OH-^{13}CHO	
A	18259.5	109.4	4.5 ± 0.7	−49.5 ± 19.1
B	6472.3	−51.9	24.1 ± 0.4	−8.6 ± 11.5
C	4924.6	−21.6	3.6 ± 0.2	5.8 ± 5.6
			CH_2OH-$CH^{18}O$	
A	18087.0	101.5	−0.8 ± 0.8	−66.7 ± 19.0
B	6242.8	−49.0	24.8 ± 0.4	−7.8 ± 11.6
C	4778.5	−21.3	4.4 ± 0.1	4.8 ± 5.9

[a] From ref 6.

TABLE 3: Comparison Parameters of the Fitted Structure and Reference Structure Ref 6

	exptl r_s structure	fitted r_e structure
C=O	1.2094 ± 0.0003 Å	1.2106 Å
C−O	1.4366 ± 0.0007 Å	1.3937 Å
C−C	1.4987 ± 0.0004 Å	1.5079 Å
O−H	1.0510 ± 0.0004 Å	0.9712 Å
H_{ald}−C	1.1021 ± 0.0003 Å	1.1058 Å
H_{alc}−C	1.0930 ± 0.0003 Å	1.0897 Å
−C−C=O	122°44′ ± 2′	121°26′
−C−C−H_{ald}	115°6′ ± 2′	116°52′
−C−C−O	111°28′ ± 2′	111°59′
−C−O−H	101.34° ± 2′	105°19′
−C−C−H_{alc}	109.13° ± 1′	107°50′
−H−C−H	107°34′ ± 2′	104°56′
−H−C−O	109°39′ ± 1′	111°56′

Note that the grid step size of 30° for the 18 dimensional surface is coarse and may result is some non-smooth behavior of the potential when interpolating between ab initio data points. However, DMC, being a statistical method, is well suited to dealing with such potentials. The reader should also note that, while ϕ_1 and ϕ_2 were varied over their entire range of values,

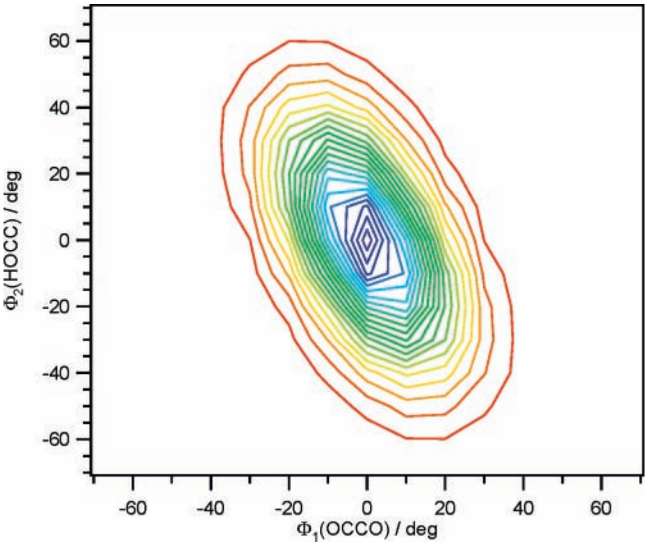

Figure 3. Contour plot the ground state wavefunction for the global minimum. Each contour represents a fall of about 5% in probability amplitude.

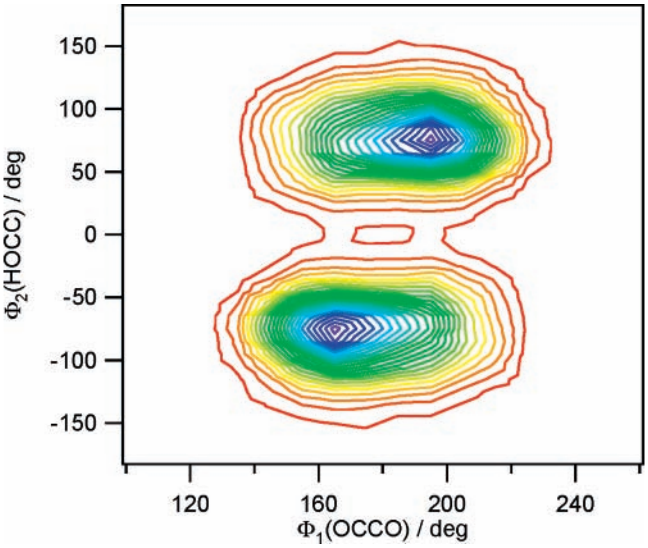

Figure 4. Contour plot the ground state wavefunction for the L2 minimum. Each contour represents a fall of about 5% in probability amplitude.

many of the remaining 16 dimensions changed little over the grid of points (e.g., bond lengths and angles). Thus interpolated energies for significantly different values of these coordinates cannot be expected to be accurate. Our 18 dimensional surface is constructed to reasonably accurately describe $V(\phi_1, \phi_2)$ but only qualitatively describe how the potential varies for the remaining 16 degrees of freedom.

Results and Discussion

The experimental rotational constants (errors less than the last significant digit given) are compared with the DMC rotational constants (error arises from the random Monte Carlo component of the simulation) for various isotopomers of the GM in Table 2. We have also included in this table the values expected for the rotational constants using perturbation theory at the B3LYP/6-31G(d,p) level as implemented in Gaussian 03.[20]

The agreement between experiment and the DMC 2-dimensional predictions is remarkable (and most likely fortuitous) considering the level of theory used and the 2-dimensional approximation. A closer examination of Table 2 reveals that the B_0 rotational constant is consistently predicted too low by about 25 MHz, which may indicate the equilibrium structure is marginally too "tight" about this axis at the B3LYP/6-31G(d,p) level. However, the 18-dimensional DMC results differed more significantly from experiment. In this case we varied the reference structural parameters to obtain the best agreement with the experimental rotational constants and obtained the geometry given in Table 3. The corresponding rotational constants using the fitted structure are also given in Table 2. The percentage average absolute error between experimental and theoretical rotational constants was reduced from 0.52 to 0.29% using the fitted structure.

A contour plot of the two-dimensional projection of the ground state wavefunction is given in Figure 3. It is evident from this figure that the hydroxy hydrogen undergoes substantial excursions away from the equilibrium position. Where the probably amplitude falls to half its maximum value Φ_2 is about ±25°, while Φ_1 travels over ±15°. Figure 3 also bears out a correlated motion between Φ_1 and Φ_2; the intramolecular H-bonded hydrogen tends to follow the electronegative carbonyl oxygen.

All attempts to localize the wavefunction about the minimum L3 failed. This was clearly due to the small barrier associated with the interconversion of L3 to GM. While a DMC calculation is not a dynamics simulation, we also recognize a relationship between the imaginary time taken for a population to migrate from one minimum down to another and the ability to isolate a system as an independent conformer, rather than detect it spectroscopically as a transient excited vibrational state. Based on the results of the two-dimensional and 18-dimensional calculations we propose that isomer L3 cannot be isolated in the gas phase.

Because of the slight energy differences between conformers L1 and L2 and the relatively low barrier between them it is difficult to predict which conformer may be isolated. By use of the 2- and 18-dimensional surfaces at the B3LYP/6-31G(d,p) level the wavefunction localizes around minima L2 and L2′ as indicated in Figure 4. However, using the energies of Senent,[10] in which isomer L1 is lower in energy, the wavefunction tends to localize about both L2 and L1 to some extent, although the projected wavefunction is somewhat difficult to interpret due to the crudeness of using a coarse grid for the PES and energies with derivatives of the energies obtained from different levels of theory. On the basis of our results, we conclude that only one other isomer of hydroxyacetaldehyde should be observable in the gas phase, and that isomer is most likely to be L2.

Acknowledgment. We thank the National University of Singapore, Faculty Research Grant, for supporting this work.

References and Notes

(1) Ehrenfreund, P.; Schutte, W. A. In *Astrochemistry: From Molecular Clouds to Planetary Systems*; Minh, Y. C., Van Dishoeck, E. F., Eds.; Sheridan Books: Chelsea, 2000; p 135.
(2) Wilfred, H. S. *Ap. J.* **2002**, *555*, L129.
(3) Bonnie, W.; Patrick, J. P.; Cherokees.L.; Hoaglund, P. H.; Wade, J. T. *Langmuir* **1996**, *12*, 2594.
(4) Galano, A.; Alvarez-Idaboy, J. R.; Ruiz-Santoy, M. E.; Vivier-Bunge, A. *J. Phys. Chem. A* **2005**, *109*, 169−180.
(5) Ochando-Pardo, M.; Nebot-Gil, I.; Gonzalez-Lafont, A.; Lluch, J. M. *J. Phys. Chem. A* **2004**, *108*, 5117.
(6) Marstokk K.-M.; Møllendal, H *J. Mol. Struct.* **1973**, *16*, 259.
(7) Marstokk K.-M.; Møllendal, H *J. Mol. Struct.* **1971**, *7*, 101.
(8) Marstokk, K.-M.; Møllendal, H. *J. Mol. Struct.* **1970**, *5*, 205.
(9) Asplala, A.; Murto, J.; Sten, P. *J. Chem. Phys.* **1986**, *106*, 339.
(10) Senent, M. L. *J. Phys. Chem. A* **2004**, *108*, 6286−6293.

(11) Liu, K.; Brown, M. G.; Carter, C.; Saykally, R. J.; Gregory, J. K.; Clary, D. C. *Nature* **1996**, *381*, 501.

(12) Clary, D. C. *J. Chem. Phys.* **2001**, *114*, 9725.

(13) Bettens, R. P. A. *J. Am. Chem. Soc.* **2003**, *125*, 584.

(14) McCoy, A. B.; Braams, B. J.; Brown, A.; Huang, X. C.; Jin, Z.; Bowman, J. M. *J. Phys. Chem. A* **2004**, *108*, 4991.

(15) Huang, X. C.; Braams, B. J.; Bowman, J. M. *J. Phys. Chem. A* **2006**, *110*, 445.

(16) Huang, X. C.; Braams, B. J.; Bowman, J. M. *J. Chem. Phys.* **2005**, *122*, 44308.

(17) Frisch, M. J.; Trucks, G. W.; Schlegel, H. B.; Scuseria, G. E.; Robb, M. A.; Cheeseman, J. R.; Zakrzewski, V. G.; Montgomery, Jr., J. A.; Stratmann, R. E.; Burant, J. C.; Dapprich, S.; Millam, J. M.; Daniels, A. D.; Kudin, K. N.; Strain, M. C.; Farkas, O.; Tomasi, J.; Barone, V.; Cossi, M.; Cammi, R.; Mennucci, B.; Pomelli, C.; Adamo, C.; Clifford, S.; Ochterski, J.; Petersson, G. A.; Ayala, P. Y.; Cui, Q.; Morokuma, K.; Malick, D. K.; Rabuck, A. D.; Raghavachari, K.; Foresman, J. B.; Cioslowski, J.; Ortiz, J. V.; Stefanov, B. B.; Liu, G.; Liashenko, A.; Piskorz, P.; Komaromi, I.; Gomperts, R.; Martin, R. L.; Fox, D. J.; Keith, T.; Al-Laham, M. A.; Peng, C. Y.; Nanayakkara, A.; Gonzalez, C.; Challacombe, M.; Gill, P. M. W.; Johnson, B.; Chen, W.; Wong, M. W.; Andres, J. L.; Gonzalez, C.; Head-Gordon, M.; Replogle, E. S.; Pople, J. A. *Gaussian 98*, revisions A.6 and A.11.2; Gaussian, Inc.: Pittsburgh, PA, 1998.

(18) Kohn, D. W.; Robles, E. S. J.; Logan, C. F.; Chen, P. *J. Phys. Chem.* 1993, *97*, 4936.

(19) Jordan, M. J. T.; Thompson, K. C.; Collins, M. A. *J. Chem. Phys.* **1995**, *102*, 5647. Thompson, K. C.; Jordan, M. J. T.; Collins, M. A. *J. Chem. Phys.* **1998**, *108*, 8302. Bettens, R. P. A.; Collins, M. A. *J. Chem. Phys.* **1999**, *111*, 816.

(20) Frisch, M. J.; Trucks, G. W.; Schlegel, H. B.; Scuseria, G. E.; Robb, M. A.; Cheeseman, J. R.; Montgomery, Jr., J. A.; Vreven, T.; Kudin, K. N.; Burant, J. C.; Millam, J. M.; Iyengar, S. S.; Tomasi, J.; Barone, V.; Mennucci, B.; Cossi, M.; Scalmani, G.; Rega, N.; Petersson, G. A.; Nakatsuji, H.; Hada, M.; Ehara, M.; Toyota, K.; Fukuda, R.; Hasegawa, J.; Ishida, M.; Nakajima, T.; Honda, Y.; Kitao, O.; Nakai, H.; Klene, M.; Li, X.; Knox, J. E.; Hratchian, H. P.; Cross, J. B.; Bakken, V.; Adamo, C.; Jaramillo, J.; Gomperts, R.; Stratmann, R. E.; Yazyev, O.; Austin, A. J.; Cammi, R.; Pomelli, C.; Ochterski, J. W.; Ayala, P. Y.; Morokuma, K.; Voth, G. A.; Salvador, P.; Dannenberg, J. J.; Zakrzewski, V. G.; Dapprich, S.; Daniels, A. D.; Strain, M. C.; Farkas, O.; Malick, D. K.; Rabuck, A. D.; Raghavachari, K.; Foresman, J. B.; Ortiz, J. V.; Cui, Q.; Baboul, A. G.; Clifford, S.; Cioslowski, J.; Stefanov, B. B.; Liu, G.; Liashenko, A.; Piskorz, P.; Komaromi, I.; Martin, R. L.; Fox, D. J.; Keith, T.; Al-Laham, M. A.; Peng, C. Y.; Nanayakkara, A.; Challacombe, M.; Gill, P. M. W.; Johnson, B.; Chen, W.; Wong, M. W.; Gonzalez, C.; Pople, J. A. *Gaussian 03*, revision B.01; Gaussian, Inc.: Pittsburgh PA, 2003.